Applied Catalysis B: Environmental 125 (2012) 215–221

Contents lists available at SciVerse ScienceDirect

Applied Catalysis B: Environmental

journal homepage: www.elsevier.com/locate/apcatb

Time evolution of surface speciation during heterogeneous photocatalysis: Gallic acid on titanium dioxide

Paula Z. Araujo[a,b], Pedro J. Morando[a,b,c], Eduardo Martínez[a,b,d], Miguel A. Blesa[a,b,d,*]

[a] Gerencia Química, Comisión Nacional de Energía Atómica, Av. General Paz 1499, 1650 San Martín, Provincia de Buenos Aires, Argentina
[b] Consejo Nacional de Investigaciones Científicas y Técnicas (CONICET), Argentina
[c] Instituto J. Sabato, Universidad Nacional de San Martín, San Martín, Provincia de Buenos Aires, Argentina
[d] Instituto de Investigación e Ingeniería Ambiental, Universidad Nacional de San Martín, San Martín, Provincia de Buenos Aires, Argentina

ARTICLE INFO

Article history:
Received 8 December 2011
Received in revised form 8 May 2012
Accepted 25 May 2012
Available online 12 June 2012

Keywords:
Gallic acid adsorption kinetics
Photocatalysis
Titanium dioxide
Surface speciation
Intermittent irradiation

ABSTRACT

Gallic acid adsorbs onto TiO_2 films deposited onto an ATR crystal in two steps, both described by the kinetic Langmuir equation, as shown by measuring the spectral changes due to adsorbed species. Both pathways lead to species with the same spectral signature.

Upon irradiation for preset times, integrated spectral absorbance profiles ($\log(A/A_0)$ vs time) for the adsorbate peaks coincides with the analogous profile of remnant concentration in solution ($\log(C/C_0)$ vs time). In our experiments, initially there are similar amounts of adsorbed and dissolved gallic acid. Hence, the rate of destruction of surface complexed gallic acid is approximately twice as large as the net rate of ligand uptake from solution. Upon irradiation, ligand surface concentration falls below equilibrium values, as also shown by plotting spectral signal intensity as a function of solution concentration.

Under intermittent irradiation, the original rates were the same, but at larger radiation doses, the overall conversion was higher. This result demonstrates that during the intervening dark periods thermal reactions contribute to the overall rate. These thermal reactions may include desorption of intermediates, dark oxidation of intermediates, and re-equilibration of the surface with increasing gallic acid surface concentration. A description of photocatalysis based in the concept of oxidation length is provided.

© 2012 Elsevier B.V. All rights reserved.

1. Introduction

The so-called heterogeneous photocatalysis (HP) is one of the advanced oxidation treatments (AOTs) that can degrade toxic organic compounds dissolved in water [1,2]. HP is a light-induced heterogeneous catalytic process through which organic molecules are oxidized on the surface of the catalyst. Photocatalysis involves the absorption of light, the wavelength of which is adequate to excite a wide band-gap semiconductor, generating an electron–hole pair; this phenomenon takes place in the time scale of 0.1 ps [3]. The fate of the pair is recombination in bulk or trapping in surface states. The typical time scale for the latter is 1 ns. Trapped pairs recombine typically in the time range of 10–100 ns. Thus, within at most 0.1 μs, the effect of the impinging photon has usually decayed to thermal energy, unless interfacial charge transfer has taken place. Photocatalysis is based on the competition of interfacial charge transfer with recombination, and charge transfer takes place typically in the 0.1–1 ms range. These time scales illustrate that usually photocatalysis takes advantage, at best, of 1% or less of the impinging photons. It is however also known that the kinetics of recombination can be arrested by trapping of the holes in surface complexes formed by chemisorption of the substrate. For instance, oxalate chemisorption generates two channels for hole trapping, the first one leading to a very fast recombination (and thus is inadequate for catalysis), and the second one decreasing the recombination rate to a time scale large than 1 ms [4]. The surface states involved in both channels can be viewed as surface complexes formed by oxalate and surface Ti atoms. Thus, the structural characterization of the species generated by chemisorption, and the knowledge of the adsorption kinetics are important in the description of the photocatalysis process.

In the study of heterogeneous catalytic processes, it is usual to establish conditions under which a steady state is reached in the surface of the catalyst. The steady state is of course dependant on the composition of the homogeneous medium, and results from the balance of fresh reagent transport to the interface, rate of transformation on the surface, and rate of mass transfer of reaction products to the bulk homogeneous medium. Slow adsorption, slow chemical reactions and slow desorption are all possible rate determining steps. Structural probes of the reactive interface under steady state

* Corresponding author at: Gerencia Química, Comisión Nacional de Energía Atómica, Av. General Paz 1499, 1650 San Martín, Provincia de Buenos Aires, Argentina. Tel.: +54 11 67727161; fax: +54 11 67727886.
E-mail address: miblesa@cnea.gov.ar (M.A. Blesa).

0926-3373/$ – see front matter © 2012 Elsevier B.V. All rights reserved.
http://dx.doi.org/10.1016/j.apcatb.2012.05.035

conditions yield time-independent results; the response of the steady state to changing bulk conditions can be explored best through independent experiments, one for each composition. On the other hand, in studies of heterogeneous photocatalytic reactions, it is common to monitor the changes in bulk composition until very large degrees of conversion (in the ideal case close to 100%) are achieved.

There is a vast wealth of information in the literature that describes the time evolution of the concentration of the pollutant in the liquid phase during the treatment, and also abundant information about the kinetics of formation and disappearance of intermediates in the course of the photocatalytic oxidation [5–7]. The oxidation of organic pollutants and its conjugated reaction, the reduction of sacrificial oxidants, take place in a thin layer adjacent to the surface; oxidation is either mediated by radicals generated from water (in particular •OH formed by hole capture by surface $^{-}$OH groups) or by direct hole capture by surface complexes [8,9]. In the case of ethanol oxidation, both pathways have been observed [10].

The intermediates, depending on their own reactivity may accumulate or may be rapidly destroyed. Important changes may take place in the surface composition during the course of the experiment: enhanced photo-adsorption of the reagent, depletion of the adsorbed reagent, changes in the speciation of the different modes of adsorption of the reagent, accumulation of reaction products or intermediates, and even changes in the effective catalytic surface area [11,12].

Most studies of aqueous HP focus on measurements of the composition of the fluid phase, without probing into the interface. In this paper we show that it is possible to obtain valuable information by monitoring both surface and bulk compositions while working at very high surface/volume ratios, conditions under which a substantial fraction of the substrate is adsorbed, and depletion of the reagent may be observed both on surface and in bulk in short time spans.

Important efforts have been devoted to the structural characterization of surface sites in various types of photocatalysts; in particular, the nature of the surface site in doped titanium dioxide. Thus, in the search for visible light activity, nitrogen doped TiO_2 has been characterized by means of X-ray diffraction, X-ray photoelectron spectroscopy (XPS), diffuse reflectance spectra and electron spin resonance, leading to the postulation of surface sites than can be described as single-electron-trapped oxygen vacancies [13]. FTIR-ATR has been used to characterize the degree of surface hydroxylation [14].

It is well known that chemisorption of organic molecules containing appropriate functional groups involves the formation of metallic complexes with the atoms in the surface of metal oxides immersed in water. In the case of TiO_2, carboxylate and phenolic groups are able to complex surface Ti(IV) ions, and these complexes mediate photocatalytic oxidation. Surface complexes have been characterized both structural and thermodynamically. Attenuated Total Reflection Infrared Spectroscopy (FTIR-ATR) [15–17] and Diffuse Reflectance FTIR [18] have been extensively used for this purpose. Studies of relevant systems include those of TiO_2 immersed in solutions containing various carboxylic acids [19–21], salicylic acid [20] catechols [22] oxalic acid [19,23], gallic acid [24] and 4,4′-bis(2-sulfostytryl)biphenyl (DSBP) [25]. Oxides and minerals other than TiO_2 have also been studied [26].

The role of surface complexes in the photocatalytic mineralization of salicylate and oxalate has been emphasized in previous work [19]. In the case of oxalate, it was possible to follow the changes of surface speciation upon irradiation, and the role played by each individual surface complex was unravelled.

Ligands containing both carboxylate and phenolic groups are important not only because of the noted affinity for Ti(IV), but also because natural organic matter (NOM) is mainly constituted by fulvic and humic acids, polymers containing many —COOH and —OH groups. In any attempt to use photocatalysis to decontaminate or disinfect natural water, NOM is an important component that may adsorb strongly and furthermore scavenge holes and •OH radicals, thus protecting other more important pollutants or bacterial cells.

Gallic acid (GA, 3,4,5-trihydroxybenzoic acid) is one of the simplest compounds that can be used as a model for NOM. Some AOTs have been used to degrade GA: catalytic oxidation by ozone [27], electrochemical oxidation [28], UV/H_2O_2, photo-Fenton and 254 nm light source [29], coupled biodegradation and ozonization [30], and vacuum-UV-photolysis of aqueous gallic acid solutions [31]. In this paper, we present a study of the photooxidation of GA on the surface of a TiO_2 film deposited onto an ATR crystal. Our first objective is to measure both the surface spectral changes and the changes in solution concentration, aiming at the comparison of the time evolution of surface and solution compositions. Gumy et al. described the time evolution of dissolved GA in illuminated solutions in contact with supported or particulate TiO_2 [32], without attempting to characterize the reactive interface.

The second objective of our work is to explore the interplay of photochemical and thermal processes. As opposed to thermally activated catalytic processes, photocatalysis takes place in (reactive) sites that are created upon impingement of photons; these sites can be described, for the oxidation reaction, as surface trapped holes. For the reduction reaction, on the other hand, electron capture takes place at the site of dioxygen adsorption. The lifetime of charge carriers being very short, thermal processes may further transform the species generated in the first hole transfer step during the comparatively long dark periods intervening between two hole trapping steps. These species may also diffuse away from the surface; in this case all further transformations are thermally activated. Not much is known about the role played by these secondary reactions in the destruction of intermediates, even though the ultimate goal of photocatalysis is the total mineralization of the substrate. We have introduced some time ago the concept of oxidation length, to describe the number of one-electron oxidation steps triggered by a single photon absorption step [33]. Here, we present experiments performed with a succession of illuminated and dark stages, the results of which suggest that thermal processes play indeed an important role in the overall reaction. Intermittent irradiation is a traditional tool to study photochemical chain reactions; for the specific case of photocatalysis, Noble and coworkers have shown that the standard intermittent illumination techniques permit a more efficient use of the impinging photons [34–36].

This approach to the assessment of the role of intermediates must be viewed as complementary to the cumbersome detection and quantification of all partially oxidised species Whereas a much less complete description is thus achieved, the experimental work is largely simplified and permits a much easier the validation of mineralization studies, focused in the analysis of the economy of photons.

A related important point in the validation of HP for pollutants destruction is the possible competition of the substrate with other dissolved species for the adsorption sites, and the effect of the dissolved species on the kinetics of charge recombination [37]. The methodology here proposed may be very useful to study these phenomena. In particular, the results also describe the possible behaviour of NOM as an irrelevant pollutant in a medium in which pollutants present at very low concentration, such as emerging contaminants, are the target [38].

We also report here measurements of the rate of GA adsorption in the dark. Mass exchange between solution and surface must necessarily be taken into account to describe HP, especially in flow reactors.

2. Experimental

2.1. Materials

Titanium dioxide P-25 from Degussa Corp. was used as received. Modal particle size is ca 25 nm and BET specific area is 51.4 $m^2\ g^{-1}$ [39].

All other reagents were analytical grade and were used without further purification. All solutions were prepared with deionized water purified by a Milli-Q system (Millipore), 18 MΩ cm^{-1} resistivity.

2.2. Methods

2.2.1. HPLC measurements

GA concentration in the supernatant solutions was measured by HPLC with UV detection, using a Spectra System UV-Vis spectrophotometer UV1000 (Thermo Finnigan LC and LC/MS Division, San Jose, CA, USA), λ = 271 nm with an Alltech 301 HPLC pump and a KoniKROM 32 (Konik-Tech. Barcelona, Spain) chromatographic data processing software. The volume of the sample loop was 200 μL with a manual injector and a flow of 1.5 mL min^{-1}. A Hamilton C18-PRP1 analytical column (reversed phase, length: 250 mm, i.d.: 4.1 mm, part size: 7 μm, pore size: 100 Å, SS, Deerfield, USA) was used. All the runs were performed at room temperature. Retention time was 7.8 min. The eluent was 5×10^{-3} mol dm^{-3} K_2HPO_4 at pH 2.5 in isocratic conditions. These HPLC experiments were unsuccessful to probe into the possible formation of intermediates in the course of the reaction.

2.2.2. FTIR-ATR procedures

The TiO_2 film was prepared by deposition from 150 μL of TiO_2 suspension (20 g dm^{-3}) on the ATR crystal surface and evaporation to dryness at room temperature. The TiO_2 layer was rinsed with water to eliminate the loosely adhered particles.

A typical experiment was performed following reference [40]. GA solutions of pH 6.15 and ionic strength $I = 1 \times 10^{-2}$ mol dm^{-3} (KCl) were stored away from light. An aliquot was placed onto the TiO_2-coated ATR crystal and the FTIR spectra were registered until equilibrium was achieved (approximately 60 min). When constant IR spectra were obtained, the supernatant remnant solution was analysed by HPLC. FTIR spectra were the average of 200 scans with 4 cm^{-1} resolution.

Next, the film was exposed to radiation from a 15 W 365 nm UV lamp and sequential IR spectra were taken. The total radiation incident on the film, measured by chemical actinometry [41] with potassium ferrioxalate was 2.4×10^{-6} Einstein s^{-1}. The average radiation per unit area was 3.3×10^{-7} Einstein $cm^{-2}\ s^{-1}$.

The evolution of the surface during photodegradation was followed in two different types of experiments:

(a) A film deposited over the ZnSe crystal was irradiated continuously for a pre-established period of time and the FTIR-ATR spectrum was recorded after irradiation; experiments for various irradiation times were performed with new films. The supernatants were analysed by HPLC.
(b) A single film was exposed to intermittent irradiation, using a light stopper; after preset irradiation times, the film was kept in the dark during 3 min before re-establishing illumination. Spectra were recorded during the dark periods.

FTIR spectra were recorded using a NICOLET MAGNA 560 instrument equipped with a liquid N_2 cooled MCT-A detector. A Spectra Tech horizontal ZnSe – ATR unit (area 10 mm × 72 mm) with an incident angle of 45° and a total number of reflections of 11 was used. The bands at 1380 cm^{-1} and 1234 cm^{-1}, assigned to ν_s (CO_2^-) and ν (Ph—O)/OH deformation vibration (COOH monomer) respectively [24], were chosen to follow the changes in GA surface concentration.

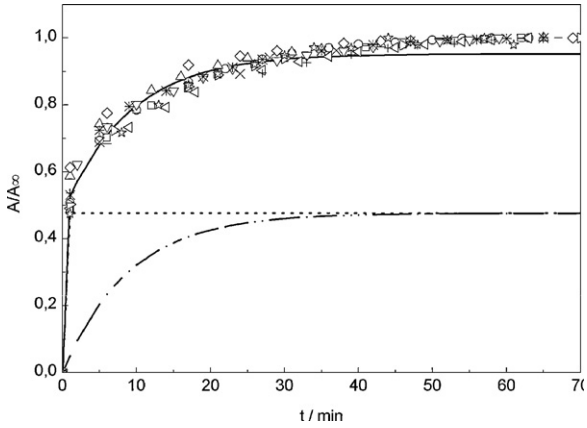

Fig. 1. Time evolution of the FTIR signal (1419:1272 cm^{-1} integrated area) (A/A_∞) for films in contact with solutions containing originally 1×10^{-4} mol L^{-1} GA at pH 6.15. Further to experimental data points, three curves are shown: (–··–) and (. . ...) Langmuir contributions; the full-line is the result of adding both contributions.

In all FTIR spectra, the background was subtracted and baseline correction was made for instrumental instabilities. In the absence of the TiO_2 film, for GA concentrations below 10^{-3} mol dm^{-3}, no appreciable IR signal was detected.

In all cases, blanks performed without the TiO_2 film demonstrated that direct GA photodegradation was always less than 5% of the total degradation.

3. Results and discussion

3.1. Kinetics of adsorption

As mentioned in the Introduction, mass transport from the solution to the interface is a necessary step in the overall photocatalytic process. Therefore, we have measured separately the kinetics of adsorption under our experimental conditions. Fig. 1 shows the time evolution of the FTIR signal (1419:1272 cm^{-1} integrated area) for films in contact with solutions containing originally 1×10^{-4} mol L^{-1} GA at pH 6.15. Mass balance demonstrates that, as an average, 48% is adsorbed when equilibrium is reached.

In replicate experiments, there is a significant scatter in the values of the absorbance reached at long times; $\sigma = \pm 0.36$, which is due to differences in the effective surface area available for adsorption in films prepared in the same conditions. However, if (A/A_∞), is plotted as a function of time, all traces overlap. Fig. 1 includes experimental data from thirteen experiments supporting this assertion. It also includes traces representing the time profile of the degree of coverage θ, which is proportional to (A/A_∞). The traces were calculating using Eq. (1), assuming that adsorption takes place through two Langmuirian rate processes with different adsorption/desorption rate constants $k_1(1)/k_{-1}(1)$ and $k_1(2)/k_{-1}(2)$, but with the same affinity constant K_L. The value for K_L was determined in a previous study of the adsorption equilibrium [24], $K_L = 5.04 \times 10^4$ $dm^3\ mol^{-1}$. The use of only one affinity constant to fit the kinetic data reflects the fact that only one surface complexation mode is identified spectroscopically [24]. The rate constants for the two Langmuirian processes yielding the better fit of the experimental points were $k_1(2) = 1.2 \times 10^3$ $dm^3\ mol^{-1}\ s^{-1}$; $k_{-1}(2) = 2.3 \times 10^{-2}\ s^{-1}$, for the slower path, and $k_1(1) = 2.07 \times 10^5$ L $mol^{-1}\ s^{-1}$; $k_{-1}(1) = 4.1\ s^{-1}$ for the faster one. The fast adsorption mode is essentially equilibrated by the time the first measurement is taken, and the quoted

figures are only lower limit values that do not influence the fitting. The slower path, on the other hand defines the shape of the experimental curve. This procedure implies that the fitting of the curve is done with only one parameter, $k_1(2)$ or $k_{-1}(2)$. A systematic deviation is apparent at long times, and is attributable to the imposed constrains, and leads to $R^2 = 92\%$.

Several possible explanations can be forwarded for the two-step adsorption kinetics. For example, transformation of adsorbed GA may take place; dimer formation through hydrogen bonding [42], or through oxidative coupling [43] has been described in the literature and the second "adsorption" process may in fact be some type of surface dimerization.[1] However, hydrogen bonding should be fast and no spectral evidence for new oxidized species is found, and we prefer to visualize the behaviour as due to two types in sites differing in kinetic availability, "readily available" and "less accessible" sites. Some type of film conditioning or evolution is probably involved, as the slower rate is too slow to describe a simple diffusive process. Such processes are known, and have been hold responsible for features such as hydrophilicity changes upon irradiation (see e.g. [4]). The values of $k_1(i)$ and $k_{-1}(i)$ were calculated assuming constant [HL]. During adsorption [HL] decreases by a factor close to two, and an average value of [HL] was used (7.5×10^{-5} mol dm^{-3}). This approximation introduces a maximum error in [HL] of 2.5×10^{-5} mol dm^{-3} in the first and last data points.

As written, this equation assumes $N_S(1) = N_S(2)$, i.e. equal total number of available sites. The fitting proved to be not very sensitive to changes in the radio $N_S(1)/N_S(2)$ around unity, and the simplest assumption was made.

In these equations, ≡Ti—OH represents generically the adsorption sites and HL stands for gallic acid.

$$\theta = \left(\frac{k_1(1)[\mathrm{HL}]}{k_1(1)[\mathrm{HL}] + k_{-1}(1)}\right)\{1 - \exp -(k_1(1)[\mathrm{HL}] + k_{-1}(1)) \times t\} + \left(\frac{k_1(2)[\mathrm{HL}]}{k_1(2)[\mathrm{HL}] + k_{-1}(2)}\right)\{1 - \exp -(k_1(2)[\mathrm{HL}] + k_{-1}(2)) \times t\} \quad (1)$$

$$\equiv\mathrm{Ti{-}OH(i)} + \mathrm{HL} \rightarrow \equiv\mathrm{Ti{-}L(i)} + \mathrm{H_2O}; \qquad k_1(\mathrm{i}) \quad (2)$$

$$\equiv\mathrm{Ti{-}L(i)} + \mathrm{H_2O} \rightarrow \equiv\mathrm{Ti{-}OH(i)} + \mathrm{HL}; \qquad k_{-1}(\mathrm{i}) \quad (3)$$

Later measurements on a series of carboxylic acids at lower degrees of coverage ([HL] ≅ 10^{-6} mol dm^{-3}) and short reaction times (t = 10 min) confirmed the operation of first order reversible kinetics, albeit in this case with participation of one type of sites only [44].

Eqs. (2) and (3) describe the first stages of the overall photooxidation reaction.

3.2. Photooxidation kinetics

For the case of weakly adsorbing species, such as phenol, adsorption does not necessarily mediate photooxidation. For these cases, even when the rate may vary with the concentration in a pseudo Langmuirian way [45], it has been proposed that the mechanism involves direct heterogeneous transfer of holes, or indirect transfer of trapped holes to the aqueous substrate [46]; the reverse charge transfer may also be important [47]. In the present case however, the time evolution of surface speciation demonstrate that surface complexes are involved.

Mineralization of organic compounds is a multistep process that may involve a variety of intermediates. For example, in the case of citric acid (HO—CR_2—COOH, with R = —CH_2COOH), Litter et al. have carried out a detailed study that shows the formation of a wide variety of intermediates, including 3-oxoglutaric acid ((HOOCCH_2)C=O) and its degradation products [48,49]. Formation of glutaric acid involves: (a) attack by h^+ or •OH; (b) decarboxylation; (c) reaction with O_2. Similarly, picloram (4-amino-3,5,6-trichloro-2-pyridincarboxylic acid) evolves through different pathways releasing CO_2. NH_3 or Cl^- [50]. For a general review on reaction pathways (for the specific case of pesticides), see Ref. [51].

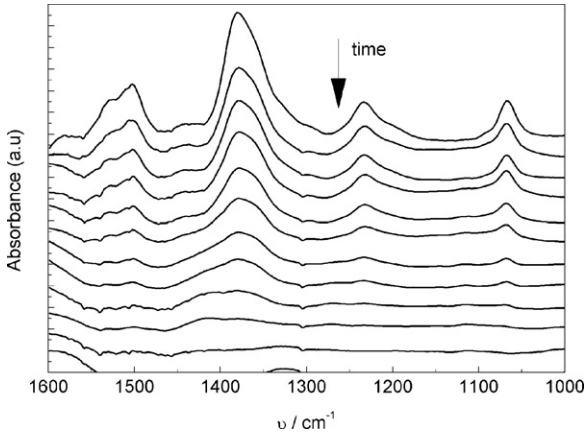

Fig. 2. ATR-FTIR spectral time evolution upon photolysis of 1800 μL GA 1×10^{-4} mol L^{-1} on the film prepared with 150 μL of 20 g L^{-1} TiO_2 suspension. From the top to bottom 0, 2, 3.5, 5, 7, 10, 13, 15, 20, 25, 35 and 45 min. See text for further details.

It is thus clear that reaction kinetics may be very complex, especially when high degrees of conversion are sought. Plots of the time evolution of remnant pollutant concentration and TOC in solution often differ, and intermediates may accumulate; see for example, [48]. In this paper, we are concerned with the time evolution of pollutant surface concentration, the time evolution of dissolved pollutant, and the comparison of both. Although the time evolution of TOC was not measured, our kinetic data (discussed below) demonstrate that intermediates are involved, but that they do not accumulate in large quantities. Our own HPLC measurements failed to demonstrate the accumulation of any intermediate, and our FTIR-ATR did not give evidence of any adsorbed intermediate. Formation of intermediates during the vacuum UV photolysis of gallic acid has been reported by Quici et al.: the rates of disappearance of gallic acid are larger in O_2-containing media, and yellow colours, due to quinoid intermediates, are seen in oxygen free media [31]. Accumulation of these intermediates may however be very low, and quantification of their time evolution very difficult, even though their rate of destruction may affect the overall rate of photooxidation. Later on we shall present a general way to take into account the existence of intermediates, and the reactions of these with either additional photogenerated strong oxidants, or with milder molecular oxidants, such as O_2.

In contrast with the extensive use of FTIR to characterize equilibrated interfaces, the use of the technique to study chemical changes is limited. FTIR has been used to follow reactions at the gas solid interface [52].

Fig. 2 shows the spectra recorded in a typical experiment, using [GA] = 1×10^{-4} mol L^{-1} at pH = 6.15 and I = 1×10^{-2} mol L^{-1} [KCl]. Every time the spectrum is recorded, the light is shut off. The intervals under light were increased as the rate decreased, and the dark intervals were ca 3 min. A monotonous decrease in the absorbance is observed, without spectral evidence of the formation of new species on the surface.

Fig. 3 (black circles) shows the time evolution of (A/A_0). Also included in Fig. 3 are data points from experiments performed irradiating continuously different individual films for different times (open circles). The same qualitative spectral features were observed

[1] We thank an anonymous reviewer for this suggestion.

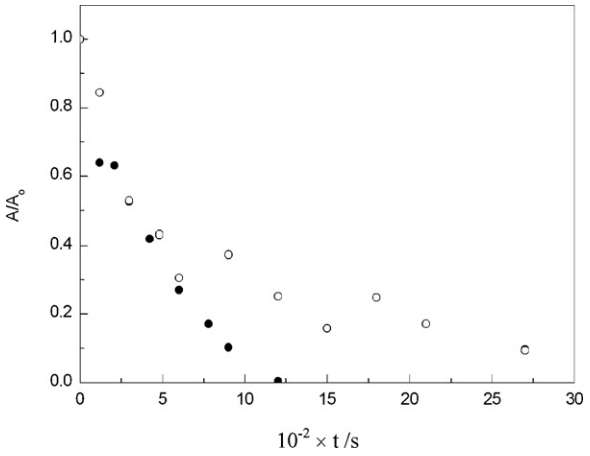

Fig. 3. Time profile of the absorbance integrated between 1419 cm^{-1} and 1272 cm^{-1}. Films prepared with 150 μL of 20 g L^{-1} TiO_2 suspension, initial GA concentration: 1×10^{-4} mol L^{-1}. (○) Each point correspond to an individual film; (●) single film experiment with intermittent irradiation.

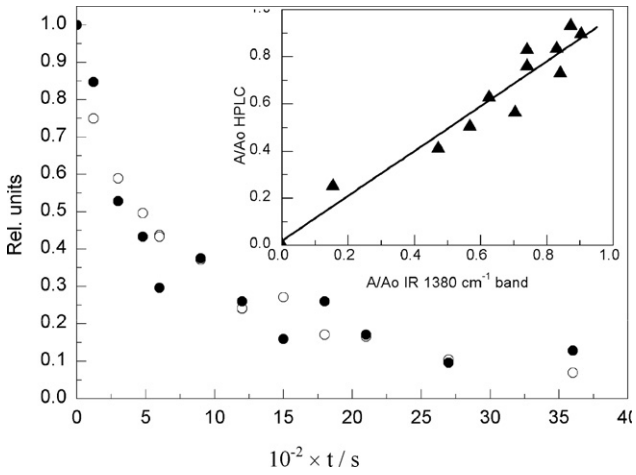

Fig. 5. Time evolution of GA concentration for the single film experiments, in relative units, (●) in the supernatant solution (HPLC); (○) on the surface (FTIR 1380 cm^{-1} band area). Inset: correlation between surface and bulk concentrations. The slope of the line is 0.952.

(spectra not shown); the rates of decrease in band intensity are initially similar but differ appreciably at longer times, as shown in Fig. 3. In this second type of experiments, residual [GA] was also measured by HPLC.

Fig. 4 shows that a first order kinetic law applies with $k = 1.03 \times 10^{-3}$ s^{-1} ($R = 96\%$) for experiments with single films and intermittent irradiation. In the experiments with a series of films irradiated continuously, the time profile deviates from first order behaviour, but in the early stages the rate are similar.

Fig. 5 compares the time evolution of GA concentration, in relative units, in the supernatant solution (as measured by the HPLC in the single film experiments) with the time evolution of the integrated FTIR 1380 cm^{-1} area band, in relative units, from Fig. 3.

The time evolution of the surface GA concentration demonstrates a deviation from adsorption equilibrium. Fig. 6 compares the degree of surface coverage calculated under equilibrium conditions with the experimental values measured by FTIR after illumination for a given time interval. The curves describe equilibrium conditions for both types of sites (upper curve) and for only one type of sites (lower curve). At $t = 0$, the data point coincides with the upper curve. Subsequent points depart from this curve to eventually reach the lower curve. It is concluded that the readily available sites remain equilibrated during photolysis, whereas the less accessible sites rapidly deplete under light. We have shown earlier that adsorption equilibration takes place slowly in the latter sites, a fact that prevents repopulation by uptake of GA from solution.

The simplest kinetic scheme to describe GA depletion is given by Eqs. (2)–(5). As stated above, this scheme ignores the obvious involvement of intermediates (HP destruction is assumed not to require further photogenerated oxidants, and that all (thermal) steps following the first oxidation step are fast; later we modify these assumptions). Note that (5) describes two parallel steps, one for each type of site, characterized by the rate constants $k_2(1)$ and $k_2(2)$. However, taking into account that the two types of sites differ only in the rate of adsorption, but not in the stability and structural features of the surface complexes, it is reasonable to assume that $k_2(1) = k_2(2)$.

$$\equiv\text{Ti—L(i)} + h\nu \rightarrow \equiv\text{Ti—P}; \qquad k_2(i) = \phi(i) I_{abs} \tag{4}$$

$$\equiv\text{Ti—P} + \text{H}_2\text{O} \rightarrow \equiv\text{Ti—OH} + \text{HP}; \qquad \text{fast} \tag{5}$$

HP represents the oxidation products of GA, I_{abs} is the absorbed light intensity, and ϕ is the quantum yield for the substrate oxidation. When k_2 becomes comparable to k_1 [HL] + k_{-1}, surface depletion is expected.

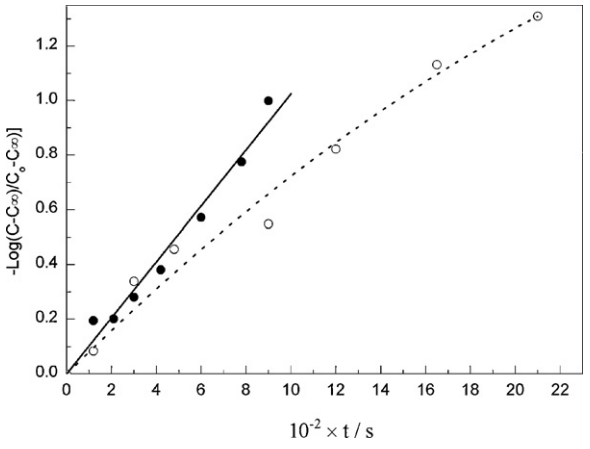

Fig. 4. First order kinetic plot of the heterogeneous photocatalytic degradation of GA from IR main band intensity: (●) single film experiment and (○) continuous irradiation experiment. Films were deposited from 150 μL of 20 g L^{-1} TiO_2 suspension. Initial GA concentration, 1.0×10^{-4} mol L^{-1}.

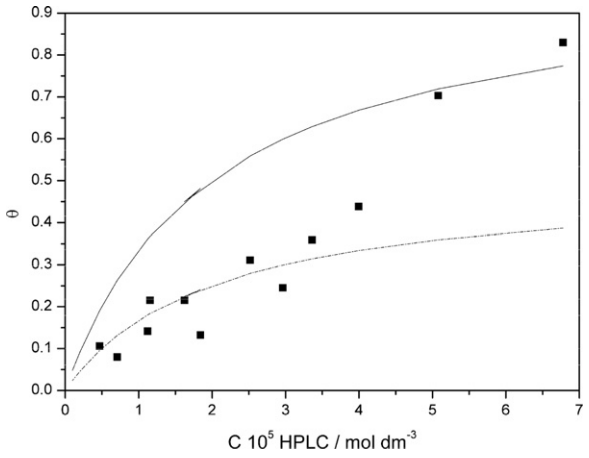

Fig. 6. Comparison of the total isotherm for GA adsorption (----) with experimental surface coverage values measured by FTIR after preset irradiation time intervals (•). The total isotherm is the sum of two Langmuirian isotherms (–··–··–). Irradiation time increases to the left.

In the general case in which comparable amounts of substrate are present in water and in the interface rather complex rate expressions result for the time evolution of dissolved and adsorbed gallic acid. The experimental data do not warrant such a detailed discussion.

Assuming that $k_2(1) = k_2(2)$, the data at short times in Fig. 6 shows an important depletion of the surface as compared to the overall adsorption isotherm. This result suggests that $k_2 \gg k_{-1}(2)$ and $k_2\{\equiv Ti{-}L(2)\} \gg k_1(2)[HL]\{\equiv Ti{-}OH(2)\}$: complexes in less accessible sites rapidly deplete. Data at longer times on the other hand show that the time evolution of sites (1) follows the equilibrium isotherm. Thus, we conclude that $k_2\{\equiv Ti{-}L(1)\} \ll k_1(1)[HL]{-}k_{-1}(1)\{\equiv Ti{-}L(1)\}$, i.e. at longer times equilibrium is maintained between readily available sites and dissolved HL. These relationships lead to the approximate identity of removed rates from solution and from surface.

Qualitatively, this behaviour is probably a general feature of film-based photo-reactors. In flow column reactors, such as SOLWATER [53], mass exchange between solution and less accessible sites is slow enough to prevent repopulation of the sites after photolytic destruction of the adsorbed molecule, and only a fraction of the total number of sites (those called here "readily available") is probably involved in the observed rate process. Detailed characteristics of the film or of the supported catalyst may have a large impact on the fraction of the total number of sites that are really used. Extrapolation of laboratory results of slurries behaviour is, at best, risky.

The oxidation of GA initiates on the illuminated surface, in a process implying direct or indirect capture of charge carriers (holes and electrons) by adsorbed GA and dioxygen. A series of subsequent steps and intermediates are required to achieve total mineralization. These intermediates are not seen by FTIR, indicating that their steady state concentrations are very low. Further evolution of the intermediates may take place in the adsorbed state, or in the liquid phase. In the former case, oxidation may be due to further heterogeneous photocatalysis, or to thermal heterogeneously catalysed reaction with dioxygen. In the second case, homogeneous thermal reactions may also be involved. No special effort was made to characterize intermediates in solution; our simple HPLC technique with optical detection at 270 nm failed to identify any of a series of possible compounds for which pure samples were available, although feeble peaks at very short elution times were seen [54].

Comparison of the two traces in Fig. 3 provides some insight into this matter. Higher rates (in terms of conversion as a function of photon doses) are observed when films are left intermittently in the dark. Continuous irradiation on the other hand leads to deviation from first order kinetics at long times (Fig. 4). Tentatively, we ascribe these results to the competition of intermediates and reactant for the charge carriers, and conclude that the intermediates are at least partially photolyzed before they are desorbed; under intermittent irradiation, the intermediates may also be destroyed during intervening dark periods. Other possible effects may be ruled out: the coupling between the rates of disappearance of dissolved GA and surface complexes (Fig. 5) does not agree with the possibility of surface coverage recovery during the dark intervals, and the lack of detection of intermediates by IR suggests that desorption of intermediates does not block the adsorption of fresh GA. The effect of O_2 on GA VUV photolysis supports our conclusion [31].

Total oxidation of GA requires 24 one-equivalent oxidation steps. Two factors define the quantum yield of HP[2]: the fraction of initial electron–hole pairs that undergo recombination, and the length of the chain established once the initial photo-generated oxidant (hole or •OH) attacks the substrate. The first factor is responsible for low quantum yields, whereas the second factor may increase the yield somewhat. Earlier [33], we have called *oxidation length* (Y) the chain length in these oxidation reactions, defined as the number of thermal oxidative steps triggered by the initial photochemical process. Seldom, if ever, the maximum possible oxidation length is obtained; more than one photon are normally necessary to complete the mineralization reaction. As stated, for GA, if total mineralization results from the absorption of one photon, $Y_{max} = 24$. We conclude that Y, while substantially lower that this limiting value, may in fact increase under intermittent irradiation.

At longer times, under steady irradiation, the degree of surface coverage by GA is low (below 0.2–0.3, for $t > 600$ s, see Fig. 3); competition with intermediates results in shorter oxidation lengths and decreasing first order rate constants. The well-known decrease in the reaction order on light intensity at high intensities [55] is another manifestation of the same phenomenon. This result suggests that an interesting approach to the optimization of the use of photon could be the design of photo reactors in which photons are directed to impinge sequentially in different areas of the reactor. Interestingly, the same type of approach is known to be unadvisable for disinfection [56,57]. Noble and coworkers have already demonstrated that a better photon efficiency is achieved by intermittent irradiation [34–36].

Chen et al. [58] have reported an increased photonic efficiency in the heterogeneous photodegradation of *o*-cresol when using intermittent irradiation; the effect was attributed to decreasing electron – hole recombination. Their results show however that the rate as a function of total deposited energy ($J\,m^{-2}$) is not very sensitive to intermittence, in contrast with our results (all our results are plotted as a function of actual irradiation time at constant I_0). The short cycle used by Chen et al. (0.1–1 s light pulses were used), as compared to the longer times used by us (several minutes under illumination, 3 min in the dark) indicate that the origin of the phenomenon observed by them is different than in our case.

The experimental k_2 value cannot be used to obtain quantum yields because only the intensity of incident radiation is known; I_{abs} is a small and unknown fraction of I_0. Furthermore, the oxidation length is also unknown. As expected, the apparent quantum yield, defined as the ratio of the initial rate to the incident photonic flux, is low, below 1%. Attempts to build a practical photooxidation reactor would require substantial improvement of the photon economy.

4. Conclusions

We have shown that the use of thin photocatalytic films deposited onto an ATR crystal permits to follow the time evolution of the surface during the photooxidation of gallic acid. Furthermore, the results may be compared with the time evolution of the remnant dissolved gallic acid in solution; comparison of both kinetic traces gives information about the interplay between adsorption and photooxidation rates. The technique also permits the easy measurement of the adsorption kinetics in the dark.

The use of intermittent irradiation, a very traditional tool in the study of photochemical chain reactions, also sheds light on the behaviour of the intermediate in the dark.

Finally, the use of the chain length concept permits to rationalize the observations without need to carry out actual detailed characterization of the possible intermediates and of their time evolution.

[2] An additional complication arises from the difficulty to establish the actual value of the absorbed light intensity (I_{abs}); normally, only the incident intensity (I_0) is known, and only apparent quantum yields are easily obtained.

Acknowledgments

Work supported by the European Commission INCO Project Cost Effective Solar Photocatalytic Technology to Water Decontamination and Disinfection in Rural Areas of Developing Countries (SOLWATER) ICA4-CT-2002-10001, by Agencia Nacional de Promoción de Ciencia y Tecnología of Argentina (PICT 06-06631) and by Comisión Nacional de Energía Atómica (CNEA), Projects P5-036-01 and P5-036-4 and by Universidad Nacional de San Martin. A doctoral fellowship by CONICET to P.Z.A. is acknowledged.

Appendix A. Supplementary data

Supplementary data associated with this article can be found, in the online version, at http://dx.doi.org/10.1016/j.apcatb.2012.05.035.

References

[1] M.R. Hoffmann, S.T. Martin, W. Choi, D. Bahnemann, Chemical Review 95 (1995) 69–96.
[2] O.M. Alfano, D. Bahnemann, A.E. Cassano, R. Dillert, R. Goslich, Catalysis Today 58 (2000) 199–230.
[3] D.E. Skinner, D.P. Colombo, J.J. Cavalieri, R.M. Bowman, The Journal of Physical Chemistry 99 (1995) 7853–7856.
[4] C.A. Mendive, PhD Dissertation Thesis, Universidad Nacional de San Martín, 2007.
[5] A.M. Peiro, J.A. Ayllon, J. Peral, X. Doménech, Applied Catalysis B 30 (2001) 359–373.
[6] J. Wiszniowski, D. Robert, J. Surmacz-Gorska, K. Miksch, J.V. Weber, Journal of Photochemistry and Photobiology A: Chemistry 152 (2002) 267–273.
[7] S.M. Kerzhentsev, C. Guillard, M. Hermann, P. Pichat, Catalysis Today 27 (1996) 215–220.
[8] J.M. Hermann, Catalysis Today 53 (1999) 115–129.
[9] J. Araña, C. Garriga i Cabo, J.M. Doña-Rodríguez, O. González-Díaz, J.A. Herrera-Melián, J. Pérez-Peña, Applied Surface Science 239 (2004) 60–71.
[10] Z. Yu, S.S.C. Chuang, Journal of Catalysis 246 (2007) 118–126.
[11] M. Takeuchi, G. Martra, S. Coluccia, M. Anpo, Journal of Physical Chemistry B 109 (2005) 7387–7391.
[12] T. Berger, O. Diwald, E. Knozinger, M. Sterrer, J.T. Yates, Physical Chemistry Chemical Physics 8 (2006) 1822–1826.
[13] Y. Wang, C. Feng, M. Zhang, J. Yang, Z. Zhang, Applied Catalysis B: Environmental 104 (2011) 268–274 (and references therein).
[14] L. Ge, J. Liu, Applied Catalysis B: Environmental 105 (2011) 289–297.
[15] S.T. Martín, J.M. Kesselman, D.S. Park, N.S. Lewis, M.R. Hoffmann, Environmental Science & Technology 30 (1996) 2535–2542.
[16] S.J. Hug, Journal of Colloid and Interface Science 188 (1997) 415–422.
[17] G.N. Ekström, A.J. McQuillan, Journal of Physical Chemistry B 103 (1999) 10562–10565.
[18] S. Kataoka, E. Lee, M.I. Tejedor-Tejedor, M.A. Anderson, Applied Catalysis B: Environmental 61 (2005) 159–163.
[19] (a) A.D. Weisz, L. García Rodenas, P.J. Morando, A.E. Regazzoni, M.A. Blesa, Catalysis Today 76 (2002) 103–112;
(b) P.Z. Araujo, C.B. Mendive, L.A. García Rodenas, P.J. Morando, A.E. Regazzoni, M.A. Blesa, D. Bahnemann, Colloids Surface A 265 (2005) 73–80;
(c) C.B. Mendive, T. Bredow, A. Feldhoff, M.A. Blesa, D. Bahnemann, Physical Chemistry Chemical Physics 11 (2009) 1794–1808.
[20] H. Hidaka, H. Honjo, S. Horikoshi, N. Serpone, Catalysis Communication 7 (2006) 331–335.
[21] M.E. Calvo, R.J. Candal, S.A. Bilmes, Environmental Science & Technology 35 (2001) 4132–4138.
[22] R. Rodriguez, M.A. Blesa, A.E. Regazzoni, Journal of Colloid and Interface Science 177 (1996) 122–131.
[23] C.B. Mendive, T. Bredow, M.A. Blesa, D.W. Bahnemann, Physical Chemistry Chemical Physics 8 (2006) 3232–3247.
[24] P.Z. Araujo, P.J. Morando, M.A. Blesa, Langmuir 21 (2005) 3470–3474.
[25] J.M. Kesselman-Truttmann, S.J. Hug, Environmental Science & Technology 33 (1999) 3171–3476.
[26] A.W.P. Vermeer, W.H. van Riemsdijk, L.K. Koopal, Langmuir 14 (1998) 2810–2819.
[27] M. Carbajo, F.J. Beltrán, F. Medina, O. Gimeno, F.J. Rivas, Applied Catalysis B: Environmental 67 (2006) 177–186.
[28] S. Mu, Synthetic Metals 139 (2003) 287–294.
[29] F.J. Benítez, F. Real, J.L. Acero, A.I. Leal, C.J. García, Hazardous Materials B 126 (2005) 31–39.
[30] D. Saroj, A. Kumar, P. Bose, V. Tare, Y. Dhopavkar, Water Research 39 (2005) 1921–1933.
[31] N. Quici, M.I. Litter, A.M. Braun, E. Oliveros, Journal of Photochemistry and Photobiology A: Chemistry 197 (2008) 306–312.
[32] D. Gumy, A.G. Rincón, R. Hajdu, C. Pulgarin, Solar Energy 80 (2006) 1376–1381.
[33] P. Mandelbaum, S.A. Bilmes, A.E. Regazzoni, M.A. Blesa, Solar Energy 65 (1999) 75–80.
[34] J.G. Sczechowski, C.A. Koval, R.D. Noble, Journal of Photochemistry and Photobiology A: Chemistry 74 (1993) 273–278.
[35] J.G. Sczechowski, C.A. Koval, R.D. Noble, Chemical Engineering Science 50 (1995) 3163–3173.
[36] N.S. Foster, C.A. Koval, J.G. Sczechowski, R.D. Noble, Journal of Electroanalytical Chemistry 406 (1996) 213–221.
[37] L.L.P. Lim, R.J. Lynch, Applied Catalysis A: General 394 (2011) 52–61.
[38] N. Miranda-García, S. Suárez, B. Sánchez, J.M. Coronado, S. Malato, M. Ignacio Maldonado, Applied Catalysis B: Environmental 103 (2011) 294–301.
[39] D. Weisz, A.E. Regazzoni, M.A. Blesa, Solid State Ionics 143 (2001) 125–130.
[40] A.D. Weisz, L. García Rodenas, P.J. Morando, M.A. Blesa, Catalysis Today 76 (2002) 103–112.
[41] J.H. Baxendale, M.K. Bridge, The Journal of Physical Chemistry 59 (1955) 783–788.
[42] J. Zhao, I.A. Khan, F.R. Fronczek, Acta Crystallographica E67 (2011) o316–o317 [doi:10.1107/S1600536811000262].
[43] J. Kawabata, Y. Okamoto, A. Kodama, T. Makimoto, T. Kasai, The Journal of Agricultural and Food Chemistry 50 (2002) 5468–5471.
[44] F. Roncaroli, M.A. Blesa, Physical Chemistry Chemical Physics 12 (2010) 9938–9944.
[45] C. Minero, Catalysis Today 54 (1999) 205–216.
[46] D. Monllor-Satoca, R. Gómez, M. González-Hidalgo, P. Salvador, Catalysis Today 129 (2007) 247–255.
[47] S. Valencia, F. Cataño, L. Ríos, G. Restrepo, J. Marín, Applied Catalysis B: Environmental 104 (2011) 300–304.
[48] N. Quici, M.E. Morgada, R.T. Gettar, M. Bolte, M.I. Litter, Applied Catalysis B: Environmental 71 (2007) 117–124.
[49] J.M. Meichtry, N. Quici, G. Mailhot, M.I. Litter, Applied Catalysis B: Environmental 102 (2011) 555–562.
[50] B. Abramović, D. Šojić, V. Despotović, D. Vione, M. Pazzi, J. Csanádi, Applied Catalysis B: Environmental 105 (2011) 191–198.
[51] H.D. Burrows, M.L. Canle, J.A. Santaballa, S. Steenken, Journal of Photochemistry and Photobiology B: Biology 67 (2002) 71–108.
[52] M.D. Hernández-Alonso, I. Tejedor-Tejedor, J.M. Coronado, M.A. Anderson, Applied Catalysis B: Environmental 101 (2011) 283–293.
[53] C. Navntoft, P. Araujo, M. Litter, M.C. Apella, D. Fernandez, M.E. Puchulu, M. del, V. Hidalgo, M. Blesa, Journal of Solar Energy Engineering 129 (2007) 127–134.
[54] P.Z. Araujo, Ph.Diss. University of San Martín, Argentina, 2008.
[55] M. Romero, J. Blanco, B. Sanchez, A. Vidal, S. Malato, A.I. Cardona, E. García, Solar Energy 66 (1999) 169–182.
[56] C. Sichel, J. Tello, M. de Cara, P. Fernández-Ibáñez, Catalysis Today 129 (2007) 152–160.
[57] A.G. Rincón, C. Pulgarin, Applied Catalysis B: Environmental 44 (2003) 263–284.
[58] H.-W. Chen, Y. Ku, A. Irawan, Chemosphere 69 (2007) 184–190.